



Effect of the steel material variability on the seismic capacity design of steel-concrete composite structures : a parametric study

Hugues Somja, Srour Nofal, Mohammed Hjiaj, Hervé Degee

► To cite this version:

Hugues Somja, Srour Nofal, Mohammed Hjiaj, Hervé Degee. Effect of the steel material variability on the seismic capacity design of steel-concrete composite structures : a parametric study. Bulletin of Earthquake Engineering, 2013, 11, pp.1099-1127. 10.1007/s10518-012-9420-5 . hal-00914616

HAL Id: hal-00914616

<https://hal.science/hal-00914616>

Submitted on 10 Dec 2013

HAL is a multi-disciplinary open access archive for the deposit and dissemination of scientific research documents, whether they are published or not. The documents may come from teaching and research institutions in France or abroad, or from public or private research centers.

L'archive ouverte pluridisciplinaire **HAL**, est destinée au dépôt et à la diffusion de documents scientifiques de niveau recherche, publiés ou non, émanant des établissements d'enseignement et de recherche français ou étrangers, des laboratoires publics ou privés.

Effect of the steel material variability on the seismic capacity design of steel-concrete composite structures : a parametric study

Hugues SOMJA¹, Srouf NOFAL¹, Mohammed HJIAJ¹, Hervé DEGEE²

¹Laboratoire de Génie Civil et Mécanique, INSA Rennes, Avenue des Buttes de Coesmes 20, F-35708 Rennes, France

²Department ArGEnCo – Structural Engineering, University of Liège, Chemin des Chevreuils 1, B-4000 Liège, Belgium
email: hugues.somja@insa-rennes.fr, mohammed.hjiaj@insa-rennes.fr, H.Degee@ulg.ac.be

ABSTRACT: Modern seismic codes recommend the design of ductile structures able to absorb seismic energy through high plastic deformation. Since seismic ductile design relies on an accurate control of plastic hinges formation, which mainly depends on the distribution of plastic resistances of structural elements, efficiency of the design method strongly depends on the actual mechanical properties of materials. The objective of the present contribution is therefore to assess the impact of material variability on the performance of capacity-designed steel-concrete composite moment resisting frames.

KEY WORDS: Steel-concrete composite structures; Material properties variability; Seismic design; capacity design.

1 GENERAL CONTEXT AND OBJECTIVES

Modern seismic codes, such as Eurocode 8 or FEMA 350, recommend designing ductile structures in such way seismic energy is absorbed through large plastic deformation of pre-defined zones.

In the current European standards, the possibility to exploit plastic resources is translated in lowered values of design seismic actions by the use of the so-called behavior factor q . In order to optimize the energy dissipation, structural plastic deformation under earthquake action must occur in such a way to involve a large number of structural elements. The localization of plastic hinges in pre-defined zones (i.e. "critical regions") along with the objective to develop efficient global energy dissipation mechanisms are obtained through a proper design methodology called "capacity design" and an appropriate definition of structural detailing. The global dissipative mechanism should develop without significant loss of the overall transverse stiffness of the structure and the plastic hinges should be able to keep their strength even for large lateral displacements. The capacity design consists in the definition of a hierarchy in the resistance of structural elements, providing some zones with sufficient overstrength with respect to those expected to plastically deform, ensuring that the formers remain in elastic range during the seismic event.

Since seismic ductile design relies on an accurate control of the plastic zones that mainly depends on the distribution of plastic resistances of structural elements, it is clear that the efficiency of the design method strongly depends on the actual mechanical properties of material.

On the other hand, even if lower limits of yield strength are defined in European production standards, no limitation on the upper limit is given [1]. It is also well known that, at least for low steel grades (S235, S275), measured yield strength exhibits a significant scattering and the actual resistance is often much higher than their nominal value. In Eurocode 8, this uncertainty is covered by the so-called material overstrength factor γ_{ov} . It can be assumed that this factor is correlated with the material overstrength (i.e. the ratio between the upper characteristic value and the nominal value of the yield strength). The current version of Eurocode 8, suggests to use a single value of γ_{ov} although material overstrength is known to vary with the nominal yield strength. This may lead to a variable safety level according to the steel grade and the structural configuration.

In this context, the objective of the present contribution is to assess the actual impact of material variability on the performance of capacity-designed steel-concrete composite moment resisting frames. The studies have been carried out in the frame of the RFCS European research project OPUS [2].

2 METHODOLOGY AND INPUT DATA

2.1 Methodology

The global methodology adopted for the present study involves a three-step procedure. Each of these three steps is presented in Section 3, 4 and 5, respectively. The methodology can be summarized as follows:

- Design of four composite steel-concrete structures according to the prescriptions of Eurocodes 3[3], 4 [4] and 8 [5]. The structures have the same typology (5 stories and 3 bays) the differences being the column-type (steel or composite), the steel grade, the concrete class and the seismicity level (design PGA);
- Assessment of the structures designed in the previous step assuming that materials are characterized by the nominal values of their mechanical properties. This assessment is carried out using Incremental NonLinear Dynamic Analysis (INLDA);

- Analysis of the impact of material variability on the structural behaviour. Several sets of material properties are generated according to Monte-Carlo simulations based on the statistical data obtained from steel production sites. INLDA is then performed for each material dataset.

The last step provides the input data for further statistical and probabilistic analyses. Conclusions are drawn in terms of fragility curves, probability of failure, and overstrength coefficients.

Whilst the EU research project OPUS investigated a wide array of structural typologies, the present contribution focuses on the composite moment resisting frames that were analyzed by the authors. It is worth pointing out that the conclusions of the present study have been found to hold for all other typologies considered within the project.

2.2 *Input data*

In order to have statistical mechanical data that reflects the actual European steel production, RIVA and ARCELORMITTAL have collected the mechanical properties of structural steel profiles produced in their plants considering various cross sectional geometries and steel manufacturing processes [2].

The statistical characteristics of these data sets have been used by RIVA to define a probabilistic model. Two different situations were identified, i.e. plate thicknesses under 16 mm, and plate thicknesses between 16 and 40 mm. An inter-correlated multi log-normal distribution has been assumed for the yield stress f_y , the ultimate stress f_u , and the ultimate elongation A . Sample sets of mechanical properties have then been generated based on the theoretical statistical model whose parameters have been properly calibrated. All the corresponding input data and generated sample properties are detailed in the final report of the OPUS research program [2].

The mechanical steel properties are defined by three values: the yielding stress f_y , the ultimate stress f_u and the ultimate deformation A . A simplified bilinear constitutive relationship is adopted, as shown in Figure 1:

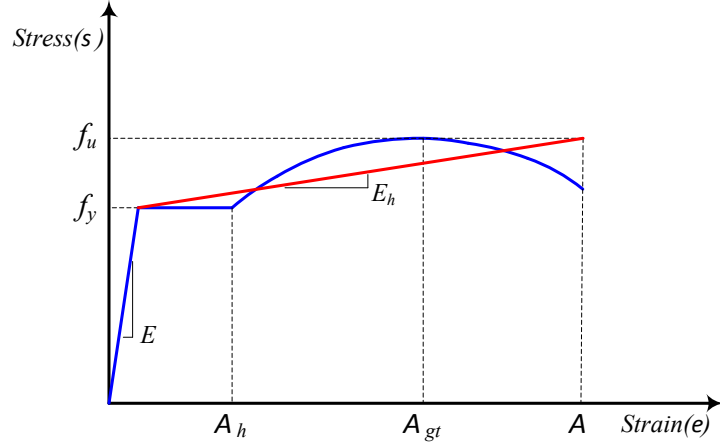


Figure 1. Simplified σ - ϵ law for steel

Mean values, standard deviations and overstrength factors deduced from statistical analysis of the mechanical properties of steel profiles and rebars obtained from the design of each structure (see section 3) are presented in Table 1.

These values give a first estimate of the overstrength γ_{ov} . Following EN1998-1-1 [5], if the statistical distribution of the yielding stress is known, the overstrength factor is computed according to equation (1):

$$\gamma_{ov,ac} = \frac{f_{yk,sup}}{f_{y,nominal}} \quad (1)$$

with $f_{yk,sup}$ being the 95% fractile of the statistical distribution and $f_{y,nominal}$ the nominal yield strength of the steel in dissipative zones. Calculated values of $\gamma_{ov,ac}$ are reported in Table 1.

Some overstrength factors obtained from mechanical characteristics appear quite high. For steel reinforcement, γ_{ov} values are in line with those given by Eurocode 8. For S355, γ_{ov} value is slightly larger, while for S235 steel grade the value appears to be very large.

It must be noted that the actual overstrength factor of S235 is nearly equal to the ratio $355/235 = 1.51$. The Eurocode 8 proposes to fulfill the strong column - weak beam principle by adopting higher steel grade for columns. In view of the results, this recommendation may look questionable. Nevertheless, the lower 5 % fractile of S355 steel is shifted from 355 MPa to 380 MPa, and the hierarchy of the resistances is preserved.

Table 1: Mean values, standard deviations and overstrength factors of steel for all case studies.

		Mean μ				Standard deviation σ				$\gamma_{ov,ac}$			
Case Study No.		1	2	3	4	1	2	3	4	1	2	3	4
Structural steel grade		S355	S355	S235	S235	S355	S355	S235	S235	S355	S355	S235	S235
Beams	profile	IPE 330	IPE 330	IPE 360	IPE 360	IPE 330	IPE 330	IPE 360	IPE 360	IPE 330	IPE 330	IPE 360	IPE 360
	f_y (Mpa)	415	415	320	320	23	23	18	18				
	f_u (Mpa)	565	565	411	410	19	19	15	15	1.28	1.28	1.49	1.49
	A (%)	25	25	25	25	2	2	2	1				
Columns	profile	HEA 360	HEA 320	HEA 450	HEA 400	HEA 360	HEA 320	HEA 450	HEA 400	HEA 360	HEA 320	HEA 450	HEA 400
	f_y (Mpa)	430	415	320	320	27	22	22	22				
	f_u (Mpa)	550	565	420	420	25	21	15	15	1.34	1.27	1.52	1.52
	A (%)	25	25	28	28	2	2	2	2				
Rebar grade		BAS 500	BAS 500	BAS 450	BAS 450	BAS 500	BAS 500	BAS 450	BAS 450	BAS 500	BAS 500	BAS 450	BAS 450
Rebars	f_y (Mpa)	561	560	525	525	22	22	17	17				
	f_u (Mpa)	671	670	630	630	20	20	19	19	1.20	1.19	1.23	1.23
	A (%)	21	21	13	13	1	1	1	1				

3 CASE STUDIES – DESIGN CONDITIONS

3.1 Structure description

Whilst the research project OPUS investigated a wide array of structural typologies, the present contribution focuses on composite steel concrete frames with either steel columns or composite columns and subjected to low as well as high seismic actions. Accordingly four possible combinations are studied (see Table 2): composite frames with steel columns (low and high seismicity) and composite frames with composite columns (low and high seismicity). All frames have the same general typology. The structure is a 5-stories / 3 bays office building, with a height of 17.5m. An intermediate beam in Y-direction allows adopting a slab's thickness of 12 cm. **The slabs are made of reinforced concrete and fully connected to the steel profile (full interaction).** The surfaces of the slabs are 21m (3 bays in the X-direction) by 24m (4 bays in the Y-direction). The dimensions of the building are given in Figure 2 and 3.

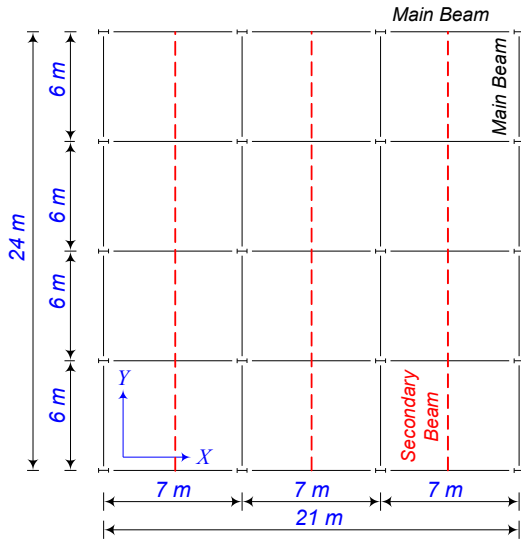


Figure 2. Plane view of the composite frames

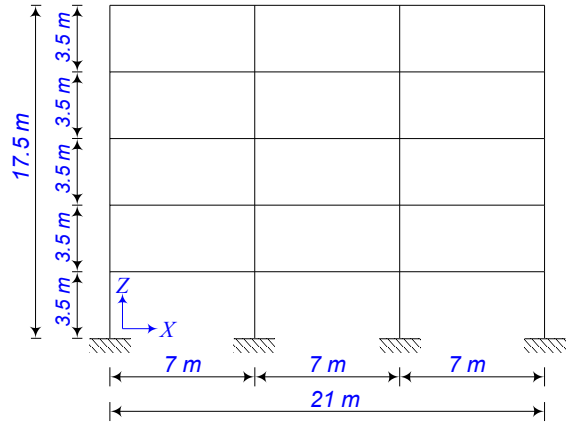


Figure 3. Elevation of the composite frame.

Table 2. Definition of the moment resisting frames.

Case	Seismicity	Columns	Structural steel	Rebars	Concrete
1	High	Steel	S355	BAS 500	C30/37
2	High	Composite	S355	BAS 500	C30/37
3	Low	Steel	S235	BAS 450	C25/30
4	Low	Composite	S235	BAS 450	C25/30

3.2 Actions

Persistent and transient design situations are defined according to EN 1991 values [6]. The live load acting on the building is chosen for a use category "office" and the other variable actions are reported in Table 3.

Table 3: Design actions for case studies

Dead Load (kN/m ²)	Live Load (kN/m ²)	Snow Load (kN/m ²)	Wind Load (kN/m ²)
5	3	1.11	1.40

Buildings are supposed to lie on a soil of type B. The importance factor γ_1 is set equal to 1. The reference peak ground acceleration (a_{gR}) is chosen equal to 0.25 g for high seismicity and 0.1g for low seismicity. The values of the parameters describing the recommended type 1 elastic response spectrum are reported

in Table 4. The corresponding elastic response spectra are represented in Figure 4. Combinations for Service Limit State (SLS) and Ultimate Limit State (ULS) are summarized in Table 5.

Table 4: Type 1 elastic response spectrum parameters

S	TB (s)	TC (s)	TD (s)
1.2	0.15	0.5	2

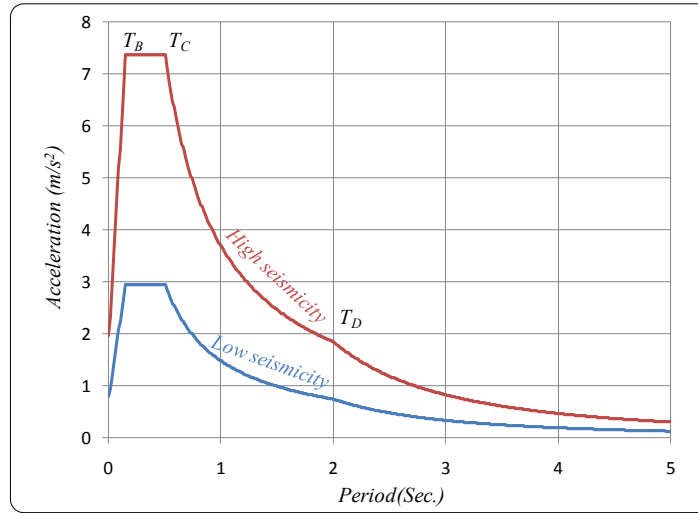


Figure 4. Elastic response spectra

Table 5: Critical load combinations at ULS and SLS

ULS	
Persistent and Transient Combination	Seismic Combination
$1.35G+1.5(S+Q)+1.05W$	$G_k + \psi_2 Q_k + E$ with $\psi_2=0.3$
SLS	
Live load combination	Wind combination
$G+Q$	$G+W$

3.3 Structural analysis

Figure 5 shows the distribution of wind and gravitational loads acting on frames for both persistent and transient design situations. The corresponding static loads are given in Table 6.

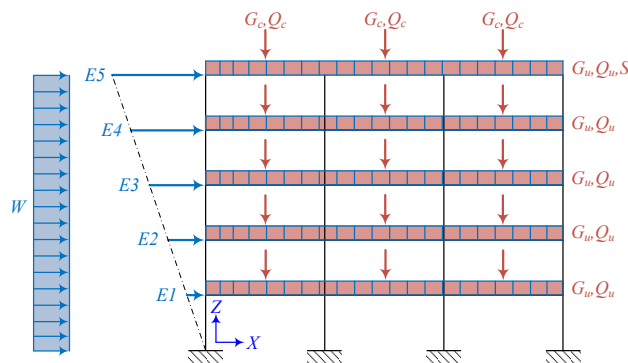


Figure 5. Distribution of actions

Table 6: Design actions

Uniform Dead Load	G_u	16.3	kN/m
Concentrated Dead Load	G_c	55.8	kN
Uniform Imposed Load	Q_u	8	kN/m
Concentrated Imposed Load	Q_c	33.5	kN
Snow load	S	6.7	kN/m
Wind load	W	8.4	kN/m

The structural analysis under seismic actions has been performed with the equivalent static lateral load method. The main seismic characteristics of the building are summarized in Table 7. The design is first performed with an initial estimate of the period given by the formula proposed in EN 1998-1:

$$T = C_t * H^{\frac{3}{4}} \quad (2)$$

with $C_t = 0.085$ and the building height, $H = 17.5\text{m}$. It is well known that this approach provides very approximate results and underestimates, in most cases, the actual period. Therefore it is conservative in terms of equivalent horizontal forces. Moreover, the coefficients are proposed for pure steel frames, while the frames considered in the present study are actually composite. The real period of the designed structure is therefore calculated and an iterative procedure is used to finally get a set of period and horizontal forces consistent with the final design. Table 7 evidences the fairly high level of conservatism of the Eurocode formula for estimating the period. Table 7 also provides the values of the second-order sensitivity coefficient θ , showing that although the structure is rather flexible, second-order effects remain limited. Indeed according to Eurocode 8, these latter can be neglected if θ is lower than 0.1.

Table 7: Main dynamic properties of the buildings

Case	Total mass (t)	Actual Period (s)	EC8 Period (s)	S_d (q included) for actual period (m/s^2)	S_d (q included) for the EC8 estimate of the period (m/s^2)	Second-order sensitivity coefficient θ
1	1900	1.64	0.727	0.561	1.265	0.048
2	1963	1.72	0.727	0.535	1.265	0.057
3	1916	1.35	0.727	0.272	0.506	0.033
4	1994	1.41	0.727	0.261	0.506	0.043

A Medium Ductility Class (DCM in EC8) has been chosen leading to a behavior factor q equal to 4. As a consequence, all beams must be at least in class 2.

Figure 5 shows the distribution of seismic design loads acting on the composite frames. The seismic forces E_i are given in Table 8 for all case studies, the remaining design loads being the same as those

given in Table 6. Axial force and bending moment diagrams for the most critical load combination at ULS are drawn in Figure 6 for case study number 1, only.

Table 9 provides the maximum bending moments and axial forces obtained from the structural analysis. As can be seen, the maximum bending moments for buildings in high and low seismicity are fairly close. This is due to the predominant effect of wind action which governs the design. Since the seismic capacity design does not take into account the origin of the forces when defining the overstrength needed for non dissipative elements, this means that all cases will be designed to resist the same level of horizontal action (due to the wind) by plastic dissipation, and this will lead to a significant overdesign for low seismicity cases.

Table 8: Seismic actions

Case Study No.	1	2	3	4
E1 (kN)	15.70	15.46	7.69	7.67
E2 (kN)	31.40	30.93	15.39	15.33
E3 (kN)	47.10	46.39	23.08	23.00
E4 (kN)	62.79	61.86	30.77	30.66
E5 (kN)	78.49	77.32	38.46	38.33

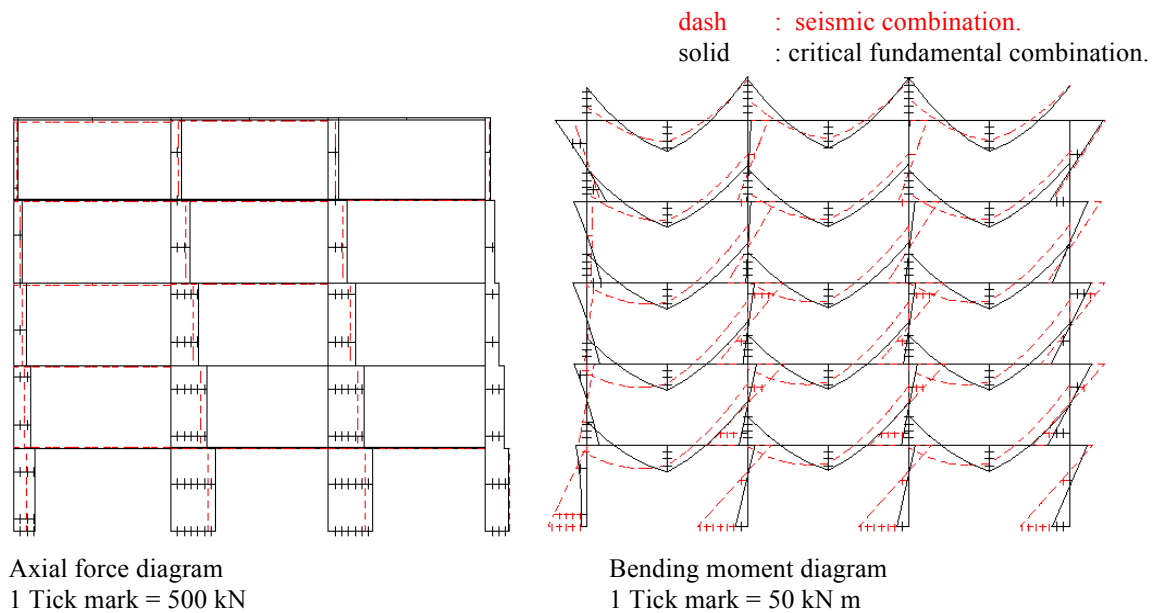


Figure 6: internal forces under seismic and static actions for the building Nr 1.

Table 9: Maximum bending moment and axial force in members of the frame

Case Study No.	1	2	3	4
----------------	---	---	---	---

Moment, $M_{Z,max}$ (kN.m)	319	326	310	317
Axial Force, N (kN)	1980	2001	1980	1998

3.4 Summary of the design

3.4.1 Cross-Section Design

Design is carried out with EN 1993, EN 1994 and EN 1998 rules. Lateral torsional buckling is supposed to be prevented for beams as well as for columns, in order to ensure a stable behavior of the members during the development of the plastic hinges. Columns are designed with the increased actions in order to respect the strong column-weak beam principle. Resulting cross sections are represented in Figure 7. The maximum ratio of design bending moment to bending moment resistance obtained for cross-sectional checks of beams and columns are given in Table 10.

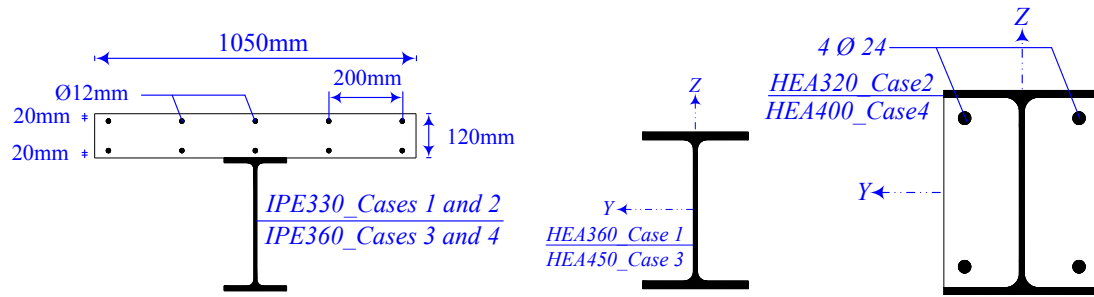


Figure 7. Structural members resulting from design.

Table 10: Maximum work-rate of beams and columns

Case Study No.		1	2	3	4
Beams - Static Actions	(EC4)	0.93	0.95	0.98	1.00
Beams - Seismic Actions	(EC8)	0.83	0.84	0.76	0.78
Columns - Static Actions	(EC4)	0.32	0.34	0.34	0.34
Columns - Seismic Actions	(EC8)	0.46	0.44	0.29	0.29

3.4.2 Global and Local Ductility Condition

In order to ensure that the collapse of the structure will occur according to a global mechanism, EN 1998-1 imposes to fulfill the "strong column – weak beam" condition at every node of the structure. This condition is expressed as:

$$\frac{\sum_c \alpha_M M_{N,Pl,Rd,c}}{\sum_b M_{pl,Rd,b}} \geq 1.3 \quad (3)$$

where \sum_c is the sum of design values of the resisting bending moments of the columns and \sum_b is that of the beams at the considered node. The coefficient α_M is equal to :

- 1 for steel columns,
- 0.9 for composite columns made of steel grades ranging between S235 and S355 inclusive.

As shown in Table 11, this condition is fulfilled at the limit for case studies in high seismicity, while a large safety margin is observed for cases in low seismicity.

Table 11. Global and local ductility condition

Case Study No.	1	2	3	4
strong column - weak beam condition	1.34	1.3	1.52	1.68

4 PRELIMINARY ASSESSMENT OF THE CASE STUDIES

A preliminary assessment of the seismic behavior of the composite frames is performed using **geometrically and materially** non linear incremental dynamic analyses with nominal values of the material properties. As suggested in EN 1998-1, seven different earthquake time-histories are adopted and the average values of the structural response obtained with these seven time-histories are considered as the representative ones. To this purpose, and according to EN1998-1 prescriptions, records of natural earthquakes or artificially generated time histories can be used. To obtain results consistent with the design seismic actions, artificial accelerograms generated from elastic response spectra through the software SIMQKE have been used. Non linear incremental dynamic analyses (INLDA) have been made using the finite element code FINELG [12].

4.1 General description of the software FINELG

FINELG is a general non linear finite element program which has been first written by F. Frey [13]. Major contributions have been made by V. de Ville de Goyet [14] who developed efficient schemes for 2D and 3D steel beams. The concrete orientation of the beam elements and the time resolution algorithm have been developed by P.Boeraeve [15]. The program is able to simulate the behaviour of structures

undergoing large displacements and moderate deformations. All beam elements are developed using a total co-rotational description. For convenience, a short description of the beam is now given. We consider a 2D Bernoulli fibre beam element with 3 nodes and 7 degrees of freedom. The total number of DOF corresponds to two rotational DOF at end nodes and 5 translational DOF (see Figure 8). The intermediate longitudinal DOF is necessary to allow to represent strong variations of the centroid position when the behaviour of the cross-section is not symmetric. Such behaviour is observed for example in concrete sections as soon as cracking occurs.

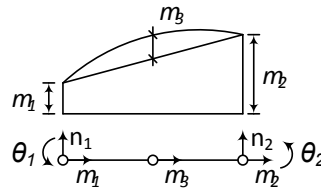


Figure 8. 3 nodes plane beam element - DOFs

As usual for fibre element, internal forces at the element nodes are computed on the basis of a longitudinal and transversal integration scheme. The integration along the beam length is performed using 2, 3 or 4 integration points (see Figure 9,a). For each longitudinal integration point LIP_i , a transversal integration is performed using the trapezoidal scheme. The section is divided into layers (see Figure 9,b) each of which being assumed in uni-axial stress state. The state of strain and stress is computed at each integration point TIP_j .

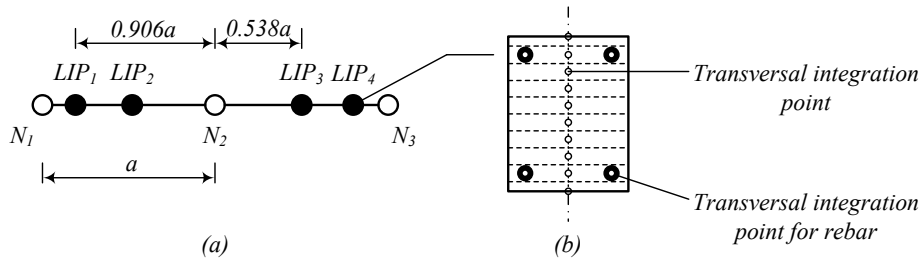


Figure 9. Integration scheme : (a) longitudinal integration with 4-point Gauss scheme; (b) transversal integration with trapezoidal scheme.

The software can be used for both static and dynamic non linear analyses. FINELG has been extensively validated for static non linear analyses. Development and validation of non linear dynamic analysis has been realized in the context of the joint research program DYNAMIX between University of Liège and Greisch [16]. **Dynamic computations have been re-assessed at the beginning of the OPUS project [2].**

4.2 INLDA analysis and definition of the structural capacity

A first assessment of the seismic behavior of each frame is performed by carrying out incremental non linear dynamic analyses considering nominal values of the material properties. It was observed that all buildings exhibit a similar seismic behavior. Indeed, for these highly redundant moment resisting frames, the only active failure criterion is the rotation capacity of the plastic hinges. No global instability, no local instability nor storey mechanism was observed, even for seismic action levels equal to 3 times the design level.

In the OPUS project, rotation demand and capacity were computed according to FEMA356 recommendations. The rotation demand is defined in Figure 10 for both beams and columns. The rotation capacity is estimated to be equal to 27 mrad for steel columns.

However, since no indication is given in FEMA 356 regarding composite beam capacities, a detailed study [10] has been undertaken to better estimate the rotation capacity of composite beams. This study relies on the plastic collapse mechanism model developed by Gioncu [7]. Figure 10 shows that the sagging zone is large with a significant part of it having a quasi-constant moment distribution near the joint. As a consequence, the plastic strains are low in steel as well as in concrete, and no crushing of the concrete is observed. On the contrary, the hogging zone is shorter but with high moment gradient. This results in a concentration of plastic deformations and in a more limited rotation capacity.

The ductility demand in plastic hinges is computed according to the actual position of contra-flexure point. Rotations of plastic hinges (θ_{b1} and θ_{b2}) in beams are calculated as follows,

$$\theta_{b1} = \theta_{c1} + \frac{(v_1 - v_3)}{L_1} \quad (4)$$

$$\theta_{b2} = \theta_{c2} + \frac{(v_1 - v_2)}{L_2} \quad (5)$$

where v_1 , v_2 and v_3 are defined in Figure 10.

The resisting moment rotation curve in the hogging zone is determined by using an equivalent standard beam (see Figure 11.a) as commonly suggested in many references (Spangemacher and Sedlacek [17] and Gioncu and Petcu [18],[19]).

A simply supported beam is subjected to a concentrated load at mid span. The post-buckling behavior is determined based on plastic collapse mechanisms (see Figure 11). Two different plastic mechanisms are considered (in-plane and out-of-plane buckling, see Figure 11.c and d respectively). The behavior is finally governed by the less dissipative mechanism (see Figure 11.b).

Elastic and hardening branches of the $M-\theta$ curve have been determined using a multi-fiber beam model. When the hardening branch intersects the $M-\theta$ curve representative of the most critical buckling mechanism (softening branch), the global behavior switches from the hardening branch to the corresponding softening branch. The equation of the softening branches can be found in [7]. The method has been implemented in MATLAB and validated against experimental results [10] and F.E. results. For OPUS buildings, it has been found from the analysis of the results that the length of the hogging zone was approximately equal to 2 m. As a consequence, an equivalent simply supported beam with $L = 4$ m is considered. The resulting $M-\theta$ curves are depicted for the composite beams of cases 1 and 2 in Figure 12 a and b.

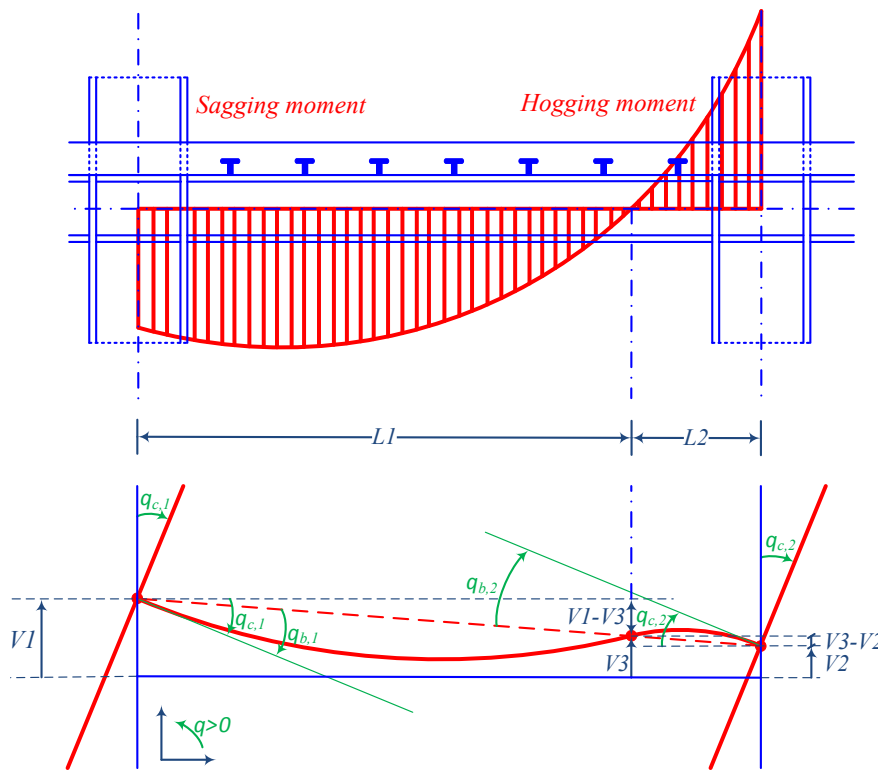


Figure 10. Typical bending moment diagram in a beam showing rotation in plastic hinges considering the exact position of the contraflexure point.

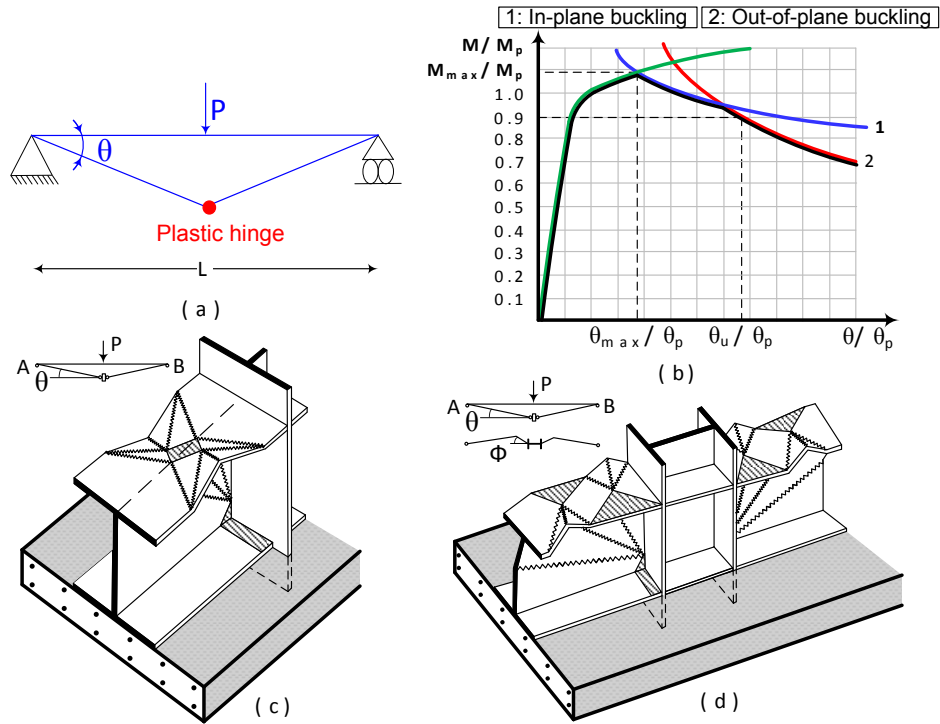


Figure 11. Model of Gioncu : (a) equivalent beam, (b) Moment rotation curve, (c) in plane buckling mechanism, (d) out of plane buckling mechanism

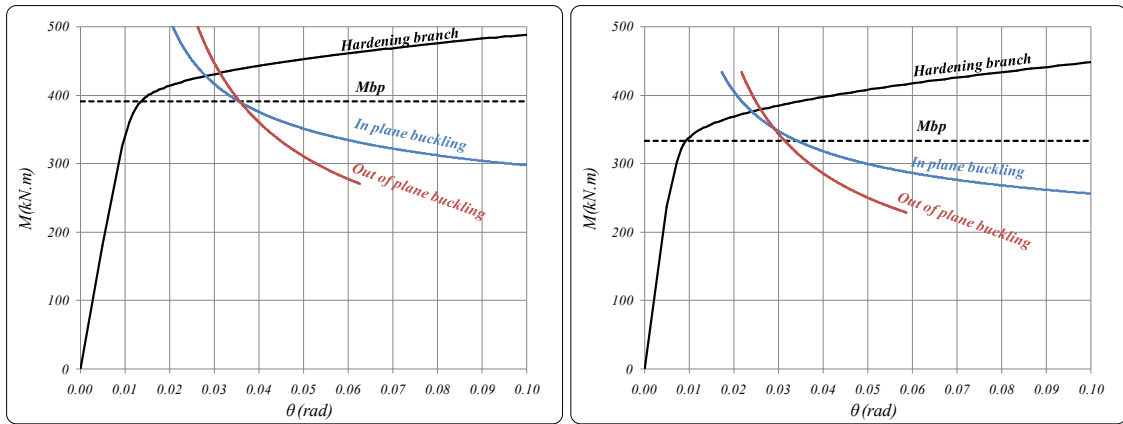


Figure 12. Moment-rotation curve of the composite beam IPE330 (a) (Case studies 1 and 2) and IPE 360 (b) (case studies 3 and 4)

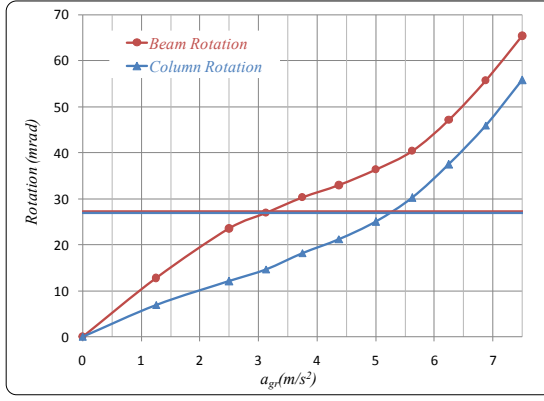
The moment-rotation curve obtained from the model of Gioncu describes the static behavior. According to Gioncu, when a plastic hinge is subjected to a cyclic loading, its behavior remains stable as long as no buckling appears. When buckling is initiated, damage accumulates from cycle to cycle. M - θ curves of the composite beam of OPUS exhibit a steep softening branch that does not allow for a long stable behavior. Consequently, in the following developments, the rotation θ_{max} corresponding to the maximum moment is considered as the maximum rotation capacity under cyclic loading.

The ultimate rotation θ_{\max} , the theoretical plastic rotation θ_p , and the ratio θ_{\max}/θ_p are reported on table 12. Since the ratio θ_{\max}/θ_p is larger for case studies 3 and 4, the relative ductility is larger, and this leads, as it will be shown in the following, to a better seismic behavior of these buildings even if they were designed for the low seismicity. While this seems to be a paradox, it is nevertheless logical. The rotation capacity is defined by the local buckling limit. Lower steel grade used for low seismicity cases is favorable for this phenomenon, as it reduces the maximum stresses attained in the steel.

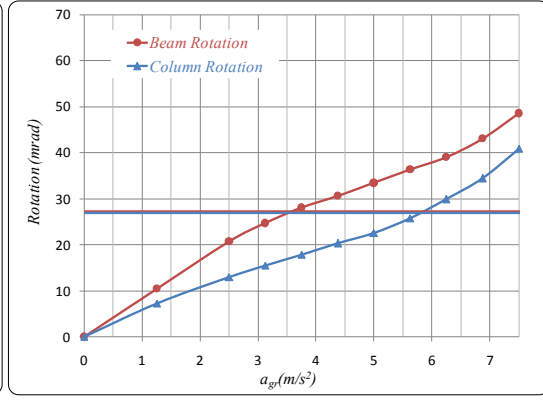
Table 12: characteristic rotations of the composite beams

Building	θ_p (mrad)	θ_{\max} (mrad)	θ_{\max}/θ_p
1 and 2	10.8	27	2.5
3 and 4	7	24	3.4

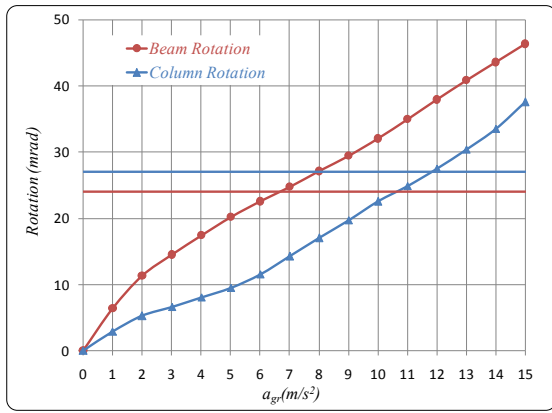
The evolution of the maximum rotation demand of the hinges in the hogging zones of the beams and at the bottom of the columns for increasing seismic acceleration a_{gR} is represented in Figure 13 for all case studies. The failure level fixed by the beam rotation criterion is considerably lower than the one fixed by the column ultimate rotation. As a consequence, the statistical analysis will focus on the ductility criterion of the beams in the hogging zone.



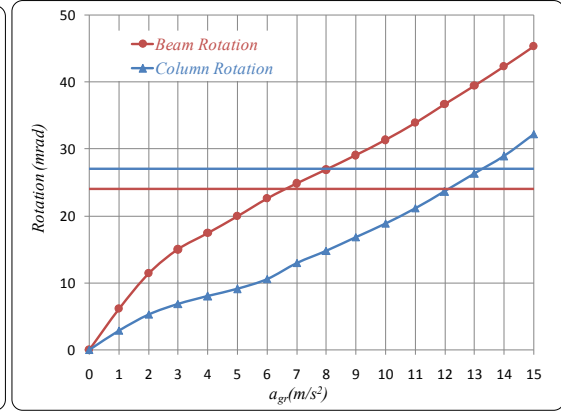
(a)



(b)



(c)



(d)

Figure 13. Results of the incremental dynamic analysis – case study 1(a), 2 (b), 3 (c), 4 (d)

4.3 Evaluation of the q factor

From the results of INLDA, the accuracy of the behavior factor values proposed by EN 1998-1 can be evaluated. In the current context, the behavior factor q can be defined as the ratio of the seismic action level leading to collapse to the seismic action level considered for an elastic design:

$$q_{\theta_u} = \frac{\lambda_{\bar{\theta}=\theta_u}}{\lambda_{e,static}} \quad (6)$$

where $\bar{\theta}$ is the mean rotation. At each hinge location, the average rotation $\bar{\theta}$ is computed considering 7 accelerograms. $\lambda_{\bar{\theta}=\theta_u}$ refers to the multiplier of the seismic action corresponding to the attainment of the ultimate rotation at one node of the structure. $\lambda_{e,static}$ is the multiplier of the equivalent static seismic forces leading to the first attainment of the plastic moment in the structure in an elastic geometrically non linear pushover analysis. This classical definition of the q -factor is compared to an expression that was proposed by Hoffmeister for the OPUS project [2]:

$$q_{\theta_u, Hoffmeister} = \frac{\lambda_{\bar{\theta}=\theta_u} * \frac{a_{s,art}}{a_{sd}}}{\lambda_{e,static}} \quad (7)$$

where $a_{s,art}$ is the acceleration of the spectrum of the accelerogram that corresponds to the fundamental period of the structure, and a_{sd} the acceleration of the elastic spectrum for the fundamental period of the structure. $q_{\theta_u, Hoffmeister}$ is computed as the mean of the q value computed for each accelerogram separately. λ_{θ_u} is the accelerogram multiplier at a maximum rotation θ_u .

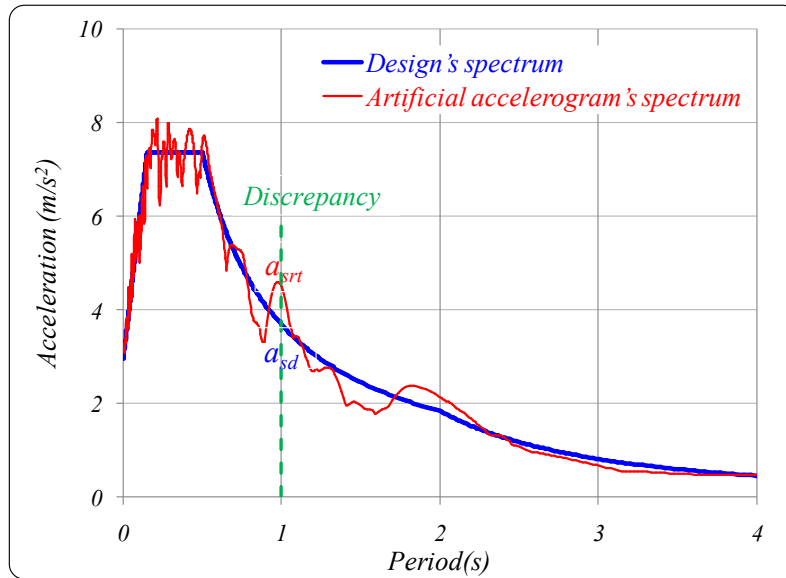


Figure 14. Discrepancy between design's spectrum and artificial accelerogram's spectrum

This alternative definition of the q -factor aims at correcting the discrepancy between the design spectrum and the spectrum corresponding to the artificial accelerogram through the factor ($a_{s,art}/a_{sd}$), see Figure 14. Both estimations of the behavior factor are presented on Table 13.

Table 13: q -factor of the different buildings - MRF

Building	Hoffmeister	classic method	Seismicity
1	2.6	3.2	High
2	3.0	3.7	High
3	5.0	5.8	Low
4	6.6	7.0	Low

The q -factors obtained by the Hoffmeister method are lower than the one obtained with the classical method. The overdesign of the buildings in low seismicity is set in evidence by the large q values. For buildings in high seismicity zones, the q factor is under 4 (value used for the design), but the intrinsic overdesign of the structures (i.e. the fact that the first plastic hinge appears for an acceleration level higher than the design level) alleviates this discrepancy.

5 ASSESSMENT OF THE STRUCTURAL BEHAVIOUR CONSIDERING MATERIAL VARIABILITY

5.1 Introduction.

The assessment of the structural behavior of buildings including material variability involves several non linear dynamic analyses of the structures considering different sets of material properties that have been generated by Monte-Carlo simulations based on the probabilistic model derived from the experimental data base(see section 2.2). The procedure produces a huge number of numerical results that must be properly analyzed in order to quantify the structural safety of the designed composite frames. In the main frame of the OPUS research, the probabilistic post-treatment of the database was performed with the aim to quantify the seismic risk associated to selected collapse criteria. The risk was quantified in terms of annual exceeding probability. This was done in a very general way in order to give pertinent results for the various collapse possibilities of the 18 different structural typologies that were analyzed. The method was established on the basis of the general approach proposed by PEER[2]. Results of the overall assessment are available in the final report of OPUS [2].

In the present contribution, limits of the application of this general method to the studied composite frames are discussed, by comparing its results against the predictions of the simple SAC/FEMA method

developed by Cornell et al. [8] and with the objective to put in evidence the relative effect of material and epistemic uncertainties.

Beside the assessment of probability of collapse based on excessive seismic demand on the dissipative elements, the effect of the material variability on the design of non dissipative elements is also investigated. To this purpose, results of the Monte-Carlo simulations are directly used to evaluate appropriate values of overstrength coefficient to be applied in the design of these non dissipative elements.

5.2 PEER general probabilistic procedure for analyzing INLDA outputs

The annual probability P_{PL} of exceeding a certain limit state (i.e. collapse at an expected performance level) within a year can be calculated using the general probabilistic approach [20] proposed by Pacific Earthquake Engineering Research centre (PEER).

For a single failure criterion considered, this method results in the following equation :

$$P_{PL}(EDP) = \int fr(IM) |dH(IM)| \quad (8)$$

with

- $P_{PL}(EDP)$ the annual probability to exceed the limit state evaluated by EDP (*Engineering Demand Parameter*), which characterize the response in terms of deformations, accelerations, induced forces or other appropriate quantities;
- $H(IM)$ is the seismic hazard function. It gives the mean annual rate of exceedance of the intensity measure of the seismic action;
- The IM (*Intensity Measure*) is obtained through conventional probabilistic seismic hazard analysis. The most commonly used IMs are PGA and spectral acceleration $S_{e,PGA}(T_0)$. It is specific to the location and design characteristics of the structure;
- $fr(IM)$ is the fragility curve. It describes the probability of exceeding the performance level for the EDP under consideration. It is given by the formula :

$$fr(IM) = \int G(EDP|DM) dG(DM|IM) \quad (9)$$

where

- DM is the damage measurement or, more appropriately, the description of structural damage associated to the selected EDPs;
- $G(EDP|DM)$ is the conditional probability of exceedance of the limit state evaluated by EDP, given the damage sustained by the structure (DM);
- $G(DM|IM)$ is the conditional probability that the Damage Measure exceeds the value DM, given the Intensity Measure.

The previous framework (8) for the assessment of structural analysis is here specified taking into account the variability of mechanical properties. In such a case, the fragility curve is given by the equation:

$$fr(IM) = \iint G(EDP|DM) dG(DM|MV, IM) dG(MV) \quad (10)$$

Where

- the material variability (MV) is explicitly considered;
- $G(DM|MV, IM)$ is the conditional probability that the Damage Measure exceeds the value DM given that the Intensity Measure equals particular values, and the material properties a given set of values;
- $G(MV)$ is the probability that the material properties equal a given set of values.

5.3 Application of PEER procedure to OPUS buildings

For each case study, nonlinear incremental dynamic analyses have been performed adopting successively the seven artificially generated accelerograms. All selected collapse criteria were then analyzed for each considered PGA level. Each of these analyses was performed considering 500 sets of material properties generated by Monte-Carlo simulations, in order to get a probabilistic distribution of the exceedance of the governing collapse criteria for each acceleration level and each time-history.

A realistic distribution of the material characteristics in the structure has been adopted. Different mechanical properties are considered for each beam B_i , while two different sets of mechanical properties are considered over the columns height, characteristics C_j , see Figure 15. A single data set is selected for all rebars, and variability of concrete material properties was not considered since it has been identified, in the preliminary assessment of section 4, that collapse was in none of the cases controlled by the failure

of the concrete material, and that the concrete stiffness had a limited effect on the global stiffness of the building.

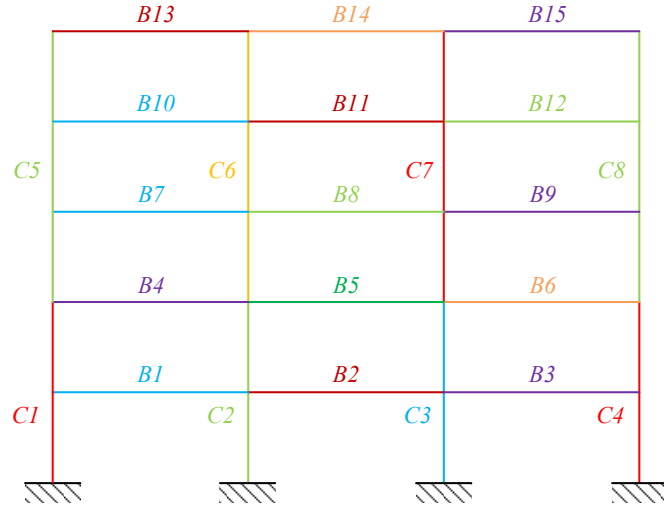


Figure 15. Distribution of the mechanical properties – Moment resisting frames.

Accordingly, 3500 numerical simulations were carried out for each case study (i.e. 7 quakes \times 500 material samples) for each considered PGA level, defining, for each collapse criterion, the damage measure (DM) for the relevant engineering demand parameter (EDP).

The output processing was executed, for each set of 500 nonlinear analyses (related to each single collapse criterion, a PGA level and accelerogram), standardizing the response using an auxiliary variable, Y_i :

$$Y_i = 100.DM_i / DM_u \quad (11)$$

where, for the specified collapse criterion, DM_i is the damage measure assumed by the EDP in the i -th analysis and DM_u is its limit value corresponding to collapse.

The new set of data was statistically analyzed evaluating the basic parameters (maximum, minimum, mean values and standard deviation) and executing the χ^2 test to check the hypothesis of Normal or Log-Normal distributions. If the χ^2 test was successful, a Normal or Log-Normal distribution was assumed. Alternatively the statistical cumulative density function was built, and completed with tails defined by suitable exponential functions [22]. The probability of failure related to each set of 500 data (related to a single collapse criterion, a PGA level and accelerogram) was simply evaluated using its cumulative density function, being :

$$fr(IM) = P[Y > 100 | IM] \quad (12)$$

For each collapse criterion and each PGA level, 7 values of collapse probability, and so 7 fragility curves, were obtained (one for each time-history). The average of those 7 fragility curves was considered as the fragility curve related to that specific collapse criterion. Fragility curve of each case study for a given collapse mode was finally integrated with European Seismic Hazard function, as described in [23], providing annual probability of failure for relevant collapse criteria for all case studies.

Before applying this procedure, results of the statistical incremental non linear dynamic analysis (SINLDA) were analyzed qualitatively. The SINLDA confirmed the conclusions established based on the computations with nominal mechanical resistances. The only active failure criterion is the ductility of the plastic hinges. No storey mechanism, nor global or local instability was observed. For the buildings under consideration, the design method of EN 1998-1 covers properly these possible collapse phenomena through the estimation of non linear effects by the amplification factor of horizontal forces, and through the local and global ductility condition defined in equation (3).

As a consequence, the study focused on the effect of the variability of the mechanical properties on the local ductility demands and capacities. Again, as in the deterministic analysis, column rotations at the column bases appeared to be lower than in beams and largely below limits computed based on FEMA rules. The hogging zone in beams appeared to be the most critical. This was also observed with nominal properties. Indeed in the sagging zone of the beams, no crushing of the concrete, nor excessive deformation of the tension flange was observed. Therefore, fragility curves were drawn only for the rotation capacity in hogging zones.

Figure 16 shows the fragility curve for case study 1 which has been constructed based on rotation demands and capacity computed from INLDA and Gioncu's model with account of the variability of mechanical characteristics. For each accelerogram, and for each multiplier, the probability of failure is computed and correspond to a point in the figure. Then the average failure probability is computed and represented by a dotted line. The fragility curve is then deduced from these average points, by adjusting a normal cumulative density function.

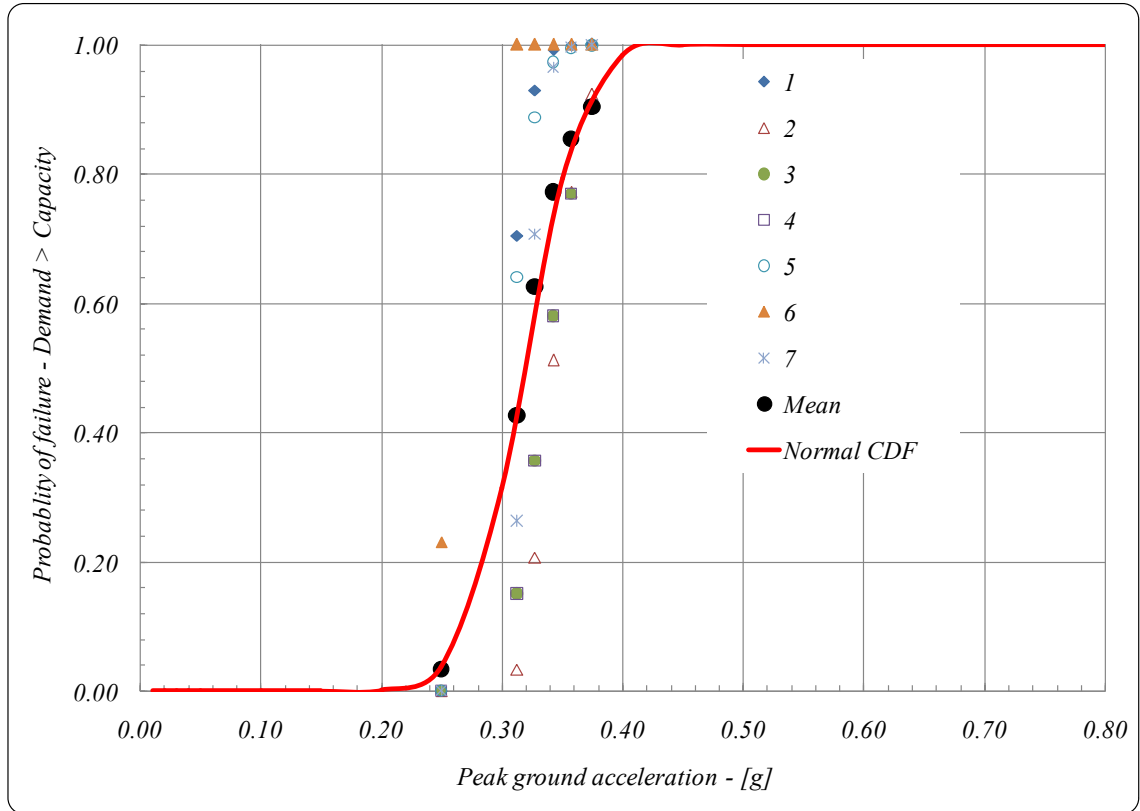


Figure 16. Fragility curve of case study Nr 1 - OPUS method.

In the OPUS procedure described above, the final fragility curve corresponds to the mean of the seven fragility curves computed for the seven different time-histories. This procedure allows to handle cases with failure defined by multiple criteria, but it mixes the uncertainty on the seismic action with the uncertainty on the material properties. In the particular case of composite moment resisting frames, since a single failure criterion was relevant, it has been considered more accurate to draw a fragility curve based on the mean of the structural response (i.e. the mean rotation) obtained with the seven accelerograms. This method is fully in line with the procedure used to define the seven accelerograms in order to get an average response spectrum fitting with the design spectrum. By doing so, the variability of the seismic action is no more included and the effect of the variability of the mechanical properties is clearly isolated.

Adopting this method does not induce significant changes in the resulting fragility curve, as it can be seen from Figure 17 for case study 1. It makes the behavior closer to the stepwise fragility curve of a deterministic system.

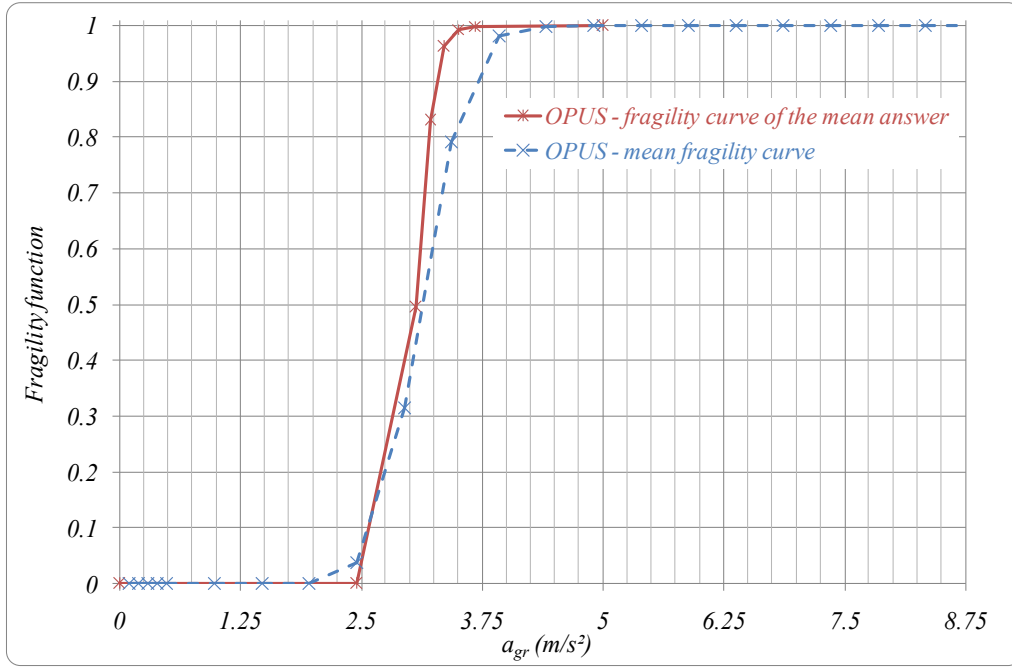


Figure 17. Comparison of the mean fragility curve to the fragility curve based on the mean rotation demand.

The mean annual probability of failure is then obtained from equation (22) adopting for the annual rate of exceedance of the reference peak ground acceleration $H(a_{gR})$ the expression proposed in EN 1998-1 :

$$H(a_{gR}) = k_0 a_{gR}^{-k} \quad (13)$$

According to the recommendations of EN 1998-1 for European seismicity, the factor k has been taken equal to 3 and k_0 was selected in order to respect the basic performance requirement of Eurocode 8 : the design seismic action should have a return period of 475 years. This results in a non-exceedance probability of $2.1 \cdot 10^{-3}$ in one year and fixes the value k_0 to 0.03097, considering $a_{gR} = 0.25$ g.

Fragility curves for the 4 case studies are drawn on Figure 18, and failure probabilities are summarized in Table 14. As a consequence of the over-resistance of buildings designed in low seismicity due to the predominance of the wind load and the improved rotation ductility of the S235 beams compared to the S355 beam it was observed that damage for low seismicity cases appears for ground accelerations that are larger than that for high seismicity cases. Accordingly, their failure probability over 1 year is very low, under $1 \cdot 10^{-5}$.

For high seismicity cases, the probability of failure of the building P_{PL} over one year is $1.1 \cdot 10^{-3}$. This value is quite high, out of the threshold ranging between 10^{-3} and 10^{-4} for this type of commonly used structure accurately designed [24]. This is consistent with the low q factor values found in section 4.3. However it must be underlined that the ULS failure criterion adopted is quite pessimistic, as it assumes that global structural failure is reached as soon as the local failure of the weakest plastic hinge occurs.

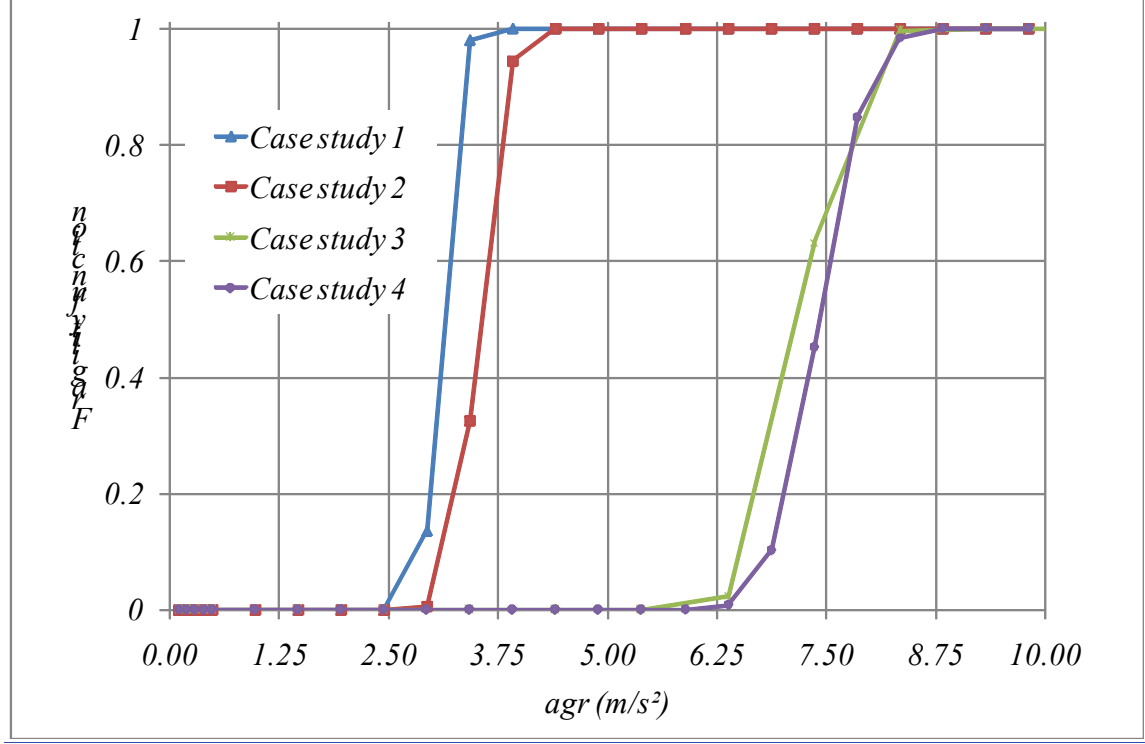


Figure 18. Fragility curves of the 4 case studies

Table 14: Failure probabilities of the 4 case studies

Return period (y)	Case study 1	Case study 2	Case study 3	Case study 4
1	1.04×10^{-3}	7.18×10^{-4}	5.40×10^{-6}	4.98×10^{-6}
50	4.96×10^{-2}	4.96×10^{-2}	2.57×10^{-4}	2.37×10^{-4}

5.4 Comparison of the OPUS procedure to the SAC/FEMA method

In order to get further insight into these results, the fragility function and the probability of failure for case study 1 have been additionally determined using the SAC/FEMA method developed by Cornell et al. [8]. A single case study is presented here, as the behavior of the 4 building does not present remarkable

differences. The SAC/FEMA framework, although being a simplified probabilistic assessment procedure, allows taking into account the epistemic uncertainties both on the demand and the capacity that were not considered in the method used in the OPUS research.

In SAC/FEMA method the fragility function is expressed as:

$$fr(agR) = P(D > C \mid agR) \quad (14)$$

with D being the demand and C the capacity related to the identified collapse criterion of the structure. For the case studies under consideration, D is the mean maximum rotation at beam end resulting from the dynamic analysis and C is the rotation capacity deduced from the model of Gioncu.

In the SAC/FEMA method, both demand and capacity are supposed to be log-normally distributed with median demand \hat{D} and median capacity \hat{C} as well as demand and capacity standard deviations β_D and β_C , respectively. The method takes also into account the epistemic uncertainties on the demand and the capacity through lognormal distributions with median equal to 1 and standard deviations equal to β_{DU} and β_{CU} .

Under these simplifying assumptions, the fragility function can be analytically expressed as:

$$fr(agR) = \Phi \left(\frac{\ln(\hat{D}) - \ln(\hat{C})}{\sqrt{\beta_D^2 + \beta_{DU}^2 + \beta_C^2 + \beta_{CU}^2}} \right) \quad (15)$$

The statistical characteristics of the demand \hat{D} and β_D are deduced from the SINLDA, based on the mean response of the 7 different accelerograms. As already stated, the rotation demand appears to be log-normally distributed. As it will be shown later, the distribution of the rotation capacity can also be accurately approximated by a lognormal distribution which justifies the applicability of the SAC/FEMA method.

The contour plots of the rotation capacity θ_{\max} are drawn as a function of $f_{y,\text{profile}}$ and $f_{y,\text{rebar}}$ (see Figure 19 (a)). As can be seen, the contour levels are nearly linear. It is therefore considered that the relationship between θ_{\max} and $f_{y,\text{profile}}, f_{y,\text{rebar}}$ is linear (Eq. (16)) :

$$\theta_{\max} = 0.0150 + 4.975 \cdot 10^{-5} f_{y, \text{profile}} - 9.022 \cdot 10^{-6} f_{y, \text{rebar}} \quad (16)$$

The above equation has been obtained using a linear regression; the difference between the linear regression and the values obtained by the direct computation is less than 1%.

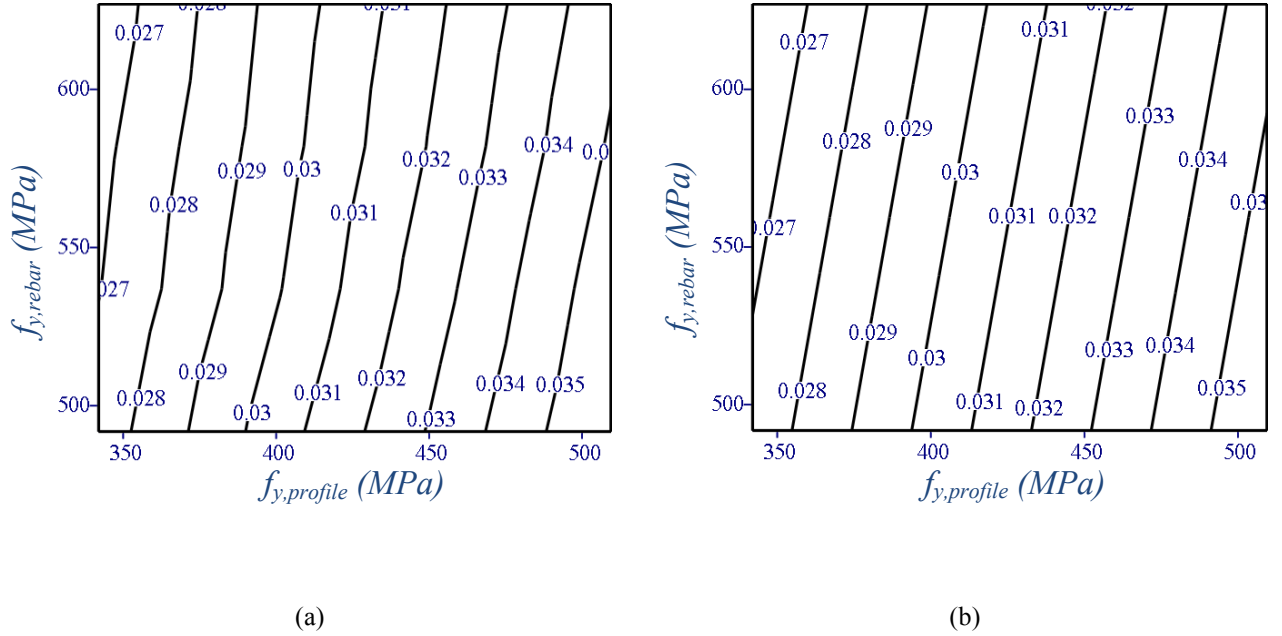


Figure 19. Evolution of θ_{\max} of the composite beam with f_y of the steel profile and of the reinforcement bar : (a) predictions of Gioncu's model (b) linear approximation

The statistical distributions of the resistances of the steel products established in OPUS are lognormal. It is possible thus to derive the distribution of θ_{\max} from these distributions using Eq. (16).

Taken into account the low variability of θ_{\max} with respect to $f_{y, \text{rebar}}$, a constant value of $f_{y, \text{rebar}}$ equal to the mean value is adopted. Consequently, the probabilistic distribution of θ_{\max} becomes a shifted log-normal distribution which depends only on $f_{y, \text{profile}}$.

Inspired by the work of Fenton [25], the distribution of θ_{\max} can then be accurately approximated by a log-normal distribution, with a mean and standard deviation of the distribution of $\ln(\theta_{\max})$, μ_z and σ_z , expressed in equations Eq. (17) and Eq. (18):

$$\sigma_z = \sqrt{\ln \left(\frac{\exp(2\mu + \sigma^2) * (\exp(\sigma^2) - 1)}{\left(\exp\left(\mu + \frac{\sigma^2}{2}\right) + \exp(0.01) \right)^2} \right) + 1} \quad (17)$$

$$\mu_z = \ln \left(\exp\left(\mu + \frac{\sigma^2}{2}\right) + \exp(0.01) \right) - \frac{\sigma_z^2}{2} \quad (18)$$

Where:

$$\mu = \text{mean} \left(\ln(4.975 * 10^{-5} f_{y,profile}) \right) = \ln(4.975 * 10^{-5}) + \text{mean} \left(\ln(f_{y,profile}) \right) \quad (19)$$

And

$$\sigma = \text{var} \left(\ln(4.975 * 10^{-5} f_{y,profile}) \right) = \text{var} \left(\ln(f_{y,profile}) \right) \quad (20)$$

The validity of this assumption is assessed by comparing its predictions against Monte Carlo calculations of θ_{\max} . The χ^2 test was positive and the above assumption has been confirmed. Moreover the error on the 5% fractile is less than 1 %. It seems therefore that the statistical distribution of the rotation capacity predicted by the Gioncu model is indeed a log-normal distribution with parameters μ_z and σ_z .

For beams of the case study 1, the median rotation capacity was found equal to 30.5 mrad, with a standard deviation $\beta_C = 0.037$. The epistemic standard deviation of the demand is chosen following the recommendations of the FEMA 350. The standard deviation of the epistemic uncertainty on the mechanical model was determined according to the differences observed between the Gioncu model and the experiments. All standard deviations are summarized in Table 15.

Table 15: Standard deviations of rotation capacity and demand

Logarithmic standard deviation	
β_D	.015
β_C	.037
β_{DU}	.2
β_{CU}	.175

SAC/FEMA fragility functions are drawn in Figure 20, considering successively a deterministic computation (with all standard deviations taken equal to 0), then with only the material uncertainties, only

the epistemic uncertainties, and finally both uncertainties. The fragility curve obtained with the OPUS approach using as demand the mean maximal rotation over the 7 accelerograms is also drawn. It coincides with the SAC/FEMA fragility curve considering only material uncertainties. This shows that the assumptions of the SAC/FEMA method are fulfilled. Both demand and capacity can indeed be considered as log-normal.

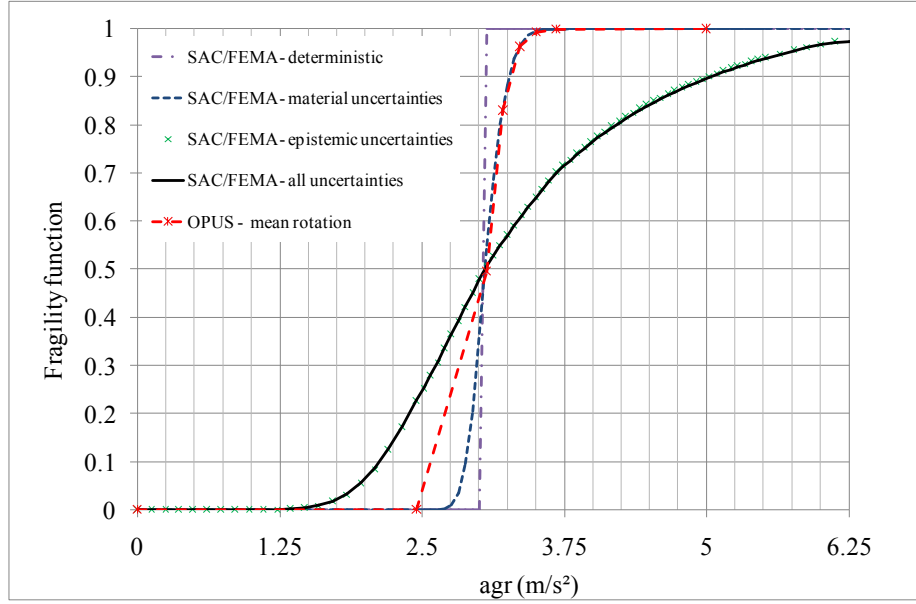


Figure 20. Fragility functions taking into account the different uncertainties

The fragility curve related to material uncertainties only is close to the one obtained with a deterministic approach whereas the fragility curve with all uncertainties coincide with the one considering only epistemic uncertainties. These two observations highlight the weak impact of the material uncertainties compared to the epistemic ones. This influence can be quantified by integrating the fragility curve with the seismic hazard $H(a_{gR})$ according to equation (22). This operation has been performed using numerical integration rather than using the simplified assumptions of the SAC/FEMA method.

The mean annual probability of failure P_{PL} computed by both methods are summarized in

Table 16. From the failure probability, the return period of failure has been computed according to (21):

$$T_L = -\frac{I}{\ln(I - P_{PL})} \quad (21)$$

Table 16: Failure probability and return period of the failure following the statistical procedure

Statistical procedure	variant	Failure probability $T_L = 1 \text{ year}$	Return period (y)
SAC/FEMA	Deterministic	1.09×10^{-3}	915
	Material uncertainties	1.08×10^{-3}	929
	Epistemic uncertainties	1.49×10^{-3}	671
	All uncertainties	1.50×10^{-3}	666
OPUS	Mean rotation	1.04×10^{-3}	957
	Mean of fragility curves	1.12×10^{-3}	894

Using the SAC/FEMA procedure, it appears that the failure probability considering only material uncertainties is nearly equal to the failure probability of the deterministic variant. The failure probability is increased by 50 % when adding the epistemic uncertainties, leading to a mean estimation of the failure probability of $1.5 \cdot 10^{-3}$.

While the fragility curves obtained with the SAC/FEMA method considering only material uncertainties and with the OPUS method considering the mean maximal rotation coincide, the estimation of the failure probability differ by 5 %. Indeed the integration of the fragility curve to get the seismic risk is performed in a different way in both methods. For SAC/FEMA method, the median response is interpolated linearly between peak ground levels considered in the non linear dynamic analysis and ten intermediate points are defined before performing the numerical integration of equation (25). Regarding the OPUS method, the fragility curve is first approximated by a normal cumulative density function. This normal function is then used to compute the fragility curve and the seismic risk H for 180 different peak ground levels covering the whole range of interest. Next, the numerical integration of equation (25) is carried out using these 180 points.

As a conclusion, the material variability has little influence on the fragility curves of the structure, compared to the effect of the epistemic uncertainties and of the variability of the seismic action. This is consistent with conclusions found for other structures that were considered within the OPUS project [2],[26],[27]. Furthermore, the results are also consistent with the observations made by other authors for reinforced concrete structures [28],[29]. The effect of the dispersion of the distribution of the material properties is very limited, and some authors even neglect it compared to the variability of the seismic action [28],[29].

5.5 Direct evaluation of the effective overstrength factors

According to capacity design principles, non dissipative elements located next to dissipative zones must be designed so that no failure occurs during plastic deformation of the ductile components. They must be able to resist an action effect defined by the general equation:

$$R_d \geq R_{d,G} + 1.1 \gamma_{ov} \Omega R_{d,E} \quad (22)$$

where $R_{d,G}$ is the action effect due to the non seismic loads included in the load combination for the seismic design situation, $R_{d,E}$ the action effect due to the seismic loads, Ω is the overstrength of the dissipative element and γ_{ov} the overstrength factor covering the effect of material variability.

In the OPUS research, the collapse probability of protected members was estimated and compared against values of collapse probabilities of dissipative members. In this approach, obtaining lower collapse probabilities for non dissipative members with respect to dissipative members corresponds to a satisfactory situation.

In this contribution, an alternative approach is followed. It consists in evaluating the overstrength factor required to avoid any failure of non dissipative members. Indeed the seismic loads and the structural response to these loads are characterized in an approximate manner with purely computational approaches. This results in a fairly large epistemic uncertainty when analyzing the seismic collapse probability. Therefore it is preferred here to stick strictly to the philosophy of the capacity design principles at local level, in order to reduce the effect of these uncertainties. In this approach, the only assumption made on the connection is that it should be designed to be rigid in such a way to be consistent with the modeling assumption of the structural model.

From the dynamic analysis performed for each of the 500 data set of material properties, it is possible to estimate the maximum forces acting on the non dissipative element. Knowing also the design action effects under non seismic ($R_{d,G}$) and seismic ($R_{d,E}$) loading, it is then possible to obtain the statistical distribution of the overstrength factor from Eq. (23):

$$\gamma_{ov} = \frac{R_{d,dyn,max} - R_{d,G}}{1.1 \Omega R_{d,E}} \quad (23)$$

where $R_{d,dyn,max}$ is the maximum load acting on the protected element, obtained from the non linear dynamic analysis. From this statistical distribution, the required overstrength factor can be deduced and compared to the code recommendations.

The study of the overstrength factor of non dissipative elements has focused on the beam-to-column joints. Equation (23) has been adapted for the specific verification of non dissipative joints in EN1998. Indeed the design criterion imposed by EN 1998-1 for non dissipative composite joints is the same than for steel joints. They should fulfill the following equation:

$$R_d \geq R_{dmin} = I. I \gamma_{ov} R_{fy} \quad (24)$$

where R_d is the resistance of the connection in accordance with EN 1993, and R_{fy} is the plastic resistance of the connected dissipative member based on the design yield stress of the material as defined in EN 1993.

The expression of γ_{ov} defined in equation (23) is then modified according to :

$$\gamma_{ov} = \frac{R_{d,dyn,max}}{I. I R_{fy}} \quad (25)$$

The effective overstrength factor needed is taken equal to the 95 % fractile of the distribution of γ_{ov} . A direct Monte Carlo computation of the maximum beam moment in hogging and in sagging has been made using in hogging the Gioncu model in order to take into account interaction between the material hardening and the plastic buckling of the flange. 500 different data sets have been considered. Then the 95 % fractile has been determined and compared to R_{dmin} . In order to assess the quality of the Monte Carlo evaluation of the 95 % fractile of the demands on the joint components, the evolution of the fractiles with increasing number of data sets is drawn in Figure 21. It appears clearly that the fractile estimation is stabilized with 500 different data sets.

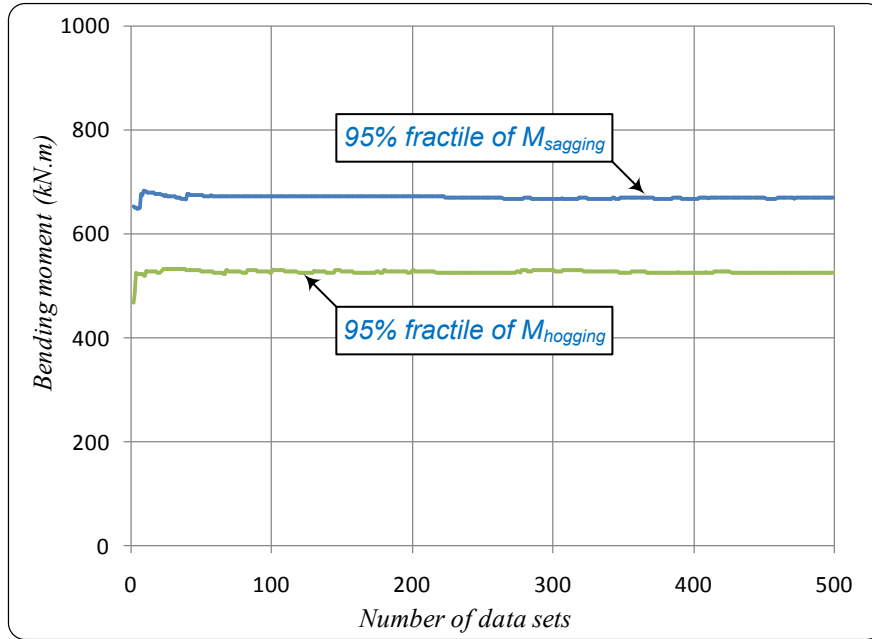


Figure 21. Fragility functions taking into account the different uncertainties

Results are presented in Table 17 for the beams of the different case studies. The effective overstrength factor found for S355 is close to the value of 1.25 proposed by the EN 1998, while the value obtained for the S235 steel is larger. These values are not surprising as they are of the same order of magnitude than the overstrength factors $\gamma_{ov,ac}$ that have been presented, see Table 1. The effective overstrength ratio appears intermediate between the values computed for the steel profile and for the reinforcement bar. These observations are in line with conclusions of other authors [30].

Table 17: Comparison of the 95 % fractile to $R_{d,min}$

Case study	Section profile	Structural steel	Rebar steel	Moment type	$R_{d,min}$ (kN m)	$R_{d,min}$ (kN m)	$\gamma_{ov,eff}$
1 and 2	IPE 330	S355	BAS 500	Hogging	525	392	1.22
				Sagging	669	495	1.23
3 and 4	IPE 360	S235	BAS 450	Hogging	531	337	1.43
				Sagging	648	415	1.42

6 CONCLUSIONS

This paper presented a study on the impact of the material variability on the seismic performances of steel-concrete composite moment resisting frames designed for low and high seismicity, carried out in the context of the European RFCS research project OPUS.

Four different buildings were designed according to the principles of capacity design and considering the prescriptions of EN 1993, EN 1994 and EN 1998.

Next, the efficiency of the ductile design, without account of the material variability, has been assessed by incremental non linear dynamic analyses (INLDA). Behaviour factors q proposed by EN 1998 have been validated.

Finally, the accuracy of the capacity design rules of EN1998, with account of the material variability of the actual production of some steel plants in Europe, has been investigated using statistical incremental non linear dynamic analyses. Sets of material properties have been generated according to Monte Carlo simulations for each building and INLDA have been performed for each data set. From these computations, the fragility curves of the buildings have been constructed, and finally, the failure probabilities were estimated by integrating the fragility curve with the seismic hazard. A brief analysis of the local overstrength demands has also been made. This consequent work has led to interesting observations, some of them requiring further research.

First, concerning the global behavior of the structures, the accuracy of the capacity design rules appears to be satisfactory :

- No storey mechanism, no local or global instability of the buildings, were observed, even for large peak ground accelerations. This observation is at first glance surprising when considering the large material overstrength that was observed for the S235 steel for example. But this overstrength corresponds to a distribution of the steel yielding stress with a mean far over 235 MPa, and with a little standard deviation. Therefore, even if dissipative members are more resistant than expected, there is no consequence since non dissipative members are also more resistant, and the statistical dispersion of the resistance around the mean value is small enough to be covered by the capacity design rules.
- It was observed that the failure was governed by the rotation capacity of the plastic hinges for moment resisting frames. It has been shown that, in all cases, the material variability has little effect on the failure criteria, and consequently on the failure probability of the case studies under

consideration. This conclusion is particularly true when comparing the effect of the material uncertainties versus the epistemic uncertainties.

- The failure probabilities are quite high, larger than the limits commonly accepted in the literature. However it must be stressed that the use of artificial accelerograms leads to larger internal forces than with natural accelerograms, and that the failure criterion adopted, using local ductility criterion as global failure indicator, is quite pessimistic.

If the large overstrength, observed for some steel grades, was demonstrated to have no effect on the global failure of the building, the same conclusion could not be held when analyzing the local overstrength specifications for non dissipative members or joints. In general, values are largely underestimated for the lower steel grade S235. However, these first conclusions should be handled with care. Indeed, the value of γ_{ov} has been determined considering only the effect of the material variability in dissipative members and not for non-dissipative zones. **For instance, in a beam-to-column joint, all joint components made of structural steel and whose resistance is not governed by instability, possess the same mean over-resistance as the plastic hinge in the beam.**

In order to take into consideration this overstrength of the non dissipative elements, one way could consist in splitting the overstrength coefficient in two coefficients:

$$\gamma_{ov} = \gamma_{ov,\mu} * \gamma_{ov,\sigma}$$

where $\gamma_{ov,\mu}$ would take into account the mean overstrength of the steel, and $\gamma_{ov,\sigma}$ the material variability around the mean. Only $\gamma_{ov,\sigma}$ would be applied to components and members made of structural steel and not subjected to instability phenomena.

As a final conclusion, the authors believe that the pessimistic observations presented in this paper should be refined with further research in order to get more insight into the effect of uncertainties on the overall behavior of structures in seismic zones. Moreover parametric studies should be extended to buildings with different numbers of storeys, different heights of the ground floor, ... Nevertheless, it seems quite clear that a new concept for overstrength is necessary in order to guarantee a safe and economic design of composite steel-concrete structures in seismic zones.

ACKNOWLEDGMENTS

The authors acknowledge the support received from European Union through the Research Fund for Coal and Steel (RFCS) as well as the support received from Belgian Fund for Research (F.R.S.-FNRS).

REFERENCES

- [1] CEN. EN 10025-1-6, Hot rolled products of non-alloys structural steel.
- [2] A. Braconi et al. OPUS Project – final report. European Union, RFCS program, 2011.
- [3] NF, EN 1993-1-1: "Design of Steel Structures – General Rules and Rules for Buildings ".October 2005
- [4] EN 1994-1-1, Eurocode 4: Design of composite steel and concrete structures, Part 1-1: General rules and rules for buildings, European Committee for Standardization, Brussels, 2004.
- [5] EN 1998-1, Eurocode 8: Design of structures for earth-quake resistance, Part 1: General rules, seismic actions and rules for buildings, European Committee for Standardization, Brussels, 2005.
- [6] NF, EN 1991-1-1: "Actions on structures; general actions - densities, self-weights, imposed loads for buildings". March 2003.
- [7] Gioncu, V, Mazzolani, F.M., “Ductility of seismic resistant steel structures”, E&FN Spon, 2002.
- [8] Federal Emergency Management Agency , “FEMA-350: Recommended Seismic Design Criteria for new steel moment frames buildings”, June 2000.
- [9] Federal Emergency Management Agency,”FEMA-356: Guideline for Seismic Rehabilitation of Buildings”, 2002.
- [10]NOFAL Srour, “Ductile seismic design of steel and steel-concrete composite structures taking into account the effect of the variability of mechanical properties of materials”, doctoral thesis, INSA de Rennes, France, 2011.
- [11]Cornell C.A., Jalayer F., Hamburger R.O., Foutch D.A., “Probabilistic Basis for 2000 SAC Federal Emergency Management Agency Steel Moment Frame Guidelines”, Journal of Structural Engineering, Vol. 128, No. 4, pp 526-533, 2002
- [12]De Ville V. ,FINELG (2003) Non linear finite element analysis program, User’s Manual Version 9.0, ULg et BEG.

- [13]Frey F. "L'analyse statique non linéaire des structures par la méthode des éléments finis et son application à la construction métallique". Doctoral thesis, Université de Liège, 1977.
- [14]De Ville V. : "L'analyse statique non linéaire par la méthode des éléments finis des structures spatiales formées de poutres à section non symétrique". Doctoral thesis, Université de Liège, 1989.
- [15]Boeraeve P.: “Contribution à l'analyse statique non linéaire des structures mixtes planes formées de poutres, avec prise en compte des effets différés et des phases de construction”. Doctoral thesis, Université de Liège, 1991.
- [16]de Ville V., Somja H., Degee H. “dynamix : calcul dynamique des structures”, 2002.
- [17]Spangemacher, R., Sedlacek, G. (1992): Zum Nachweis ausreichender Rotationsfähigkeit von Fliessgelenken bei der Anwendung des Fliessgelenkverfahrens. Stahlbau, Vol. 61, Heft 11, 329-339
- [18]Gioncu, V. and Petcu, D.: Available Rotation Capacity of Wide-Flange Beams and Columns, Part 1.Theoretical Approaches. Journal of Constructional Steel Research, 1997, 44, JCSR 1487.
- [19]V. Gioncu and D. Petcu, Available Rotation Capacity of Wide-Flange Beams and Beam–Columns, part 2. Experimental and Numerical Tests, Journal of Constructional Steel Research 43 (1997) (1–3), pp. 219–244.
- [20]Cornell CA, Krawinkler H. “Progress and challenges in seismic performance assessment.” PEER Center News 2000; 3: 2.
- [21]Tamast G., Bounds for probability in multivariate normal distribution, I.S.I. Proceedings, 203-204, 1977.
- [22]Braconi, A., Badalassi, M., Salvatore, W., Modeling of European steel qualities mechanical properties scattering and its influence on Eurocode 8 design requirements, 14th ECEE Proceedings - European Conference on Earthquake Engineering, Ohrid, Macedonia, August 30 – September 03, 2010.
- [23]Technical Commission 250/SC8, UNI-EN1998-1-1: Eurocode 8 - Design of structures for earthquake resistance. Part 1: General rules, seismic actions and rules for buildings. CEN, Brussels, 2005.
- [24]Melchers R. E., Structural reliability analysis and prediction, Ellis Horwood Limited series in civil engineering, 1987.
- [25]Fenton, L, “The sum of log-normal probability distribution in scatter transmission systems”, IRE Transactions on Communication systems, vol. 8, No. 1, pp 57-67, 1960.

- [26] Badalassi M., Braconi A., Caprili S., Salavatore W. , “Influence of steel mechanical properties on EBF seismic behaviour”, proceedings of COMPDYN 2011, Corfu, Greece, 2011
- [27] Badalassi M., Braconi A., Caprili S., Salavatore W. , “Seismic structural performance of EBF – influence of steel yielding stress limitations on collapse modes”, proceedings of Eurosteel 2011, pp 1017-1022, 2011.
- [28] Jeong S. H., Elnashai A.S., “Fragility relationships for torsionally-imbalanced buildings using three-dimensional damage characterization”, Engineering structures 29, pp 2172-2182, 2007
- [29] Kwon OS, Elnashai AS, “The effect of material and ground motion uncertainty on the seismic vulnerability curves of RC structures”, Engineering structures 28, pp289-303, 2006
- [30] Piluso V., Rizzano G., “Random material variability effects on full-strength end-plate beam-to-column joints” Journal of Constructional Steel Research, Volume 63, Issue 5, pp 658-666, 2007